Article

Journal of Biomedical Nanotechnology
Vol. 9, 1–12, 2013
www.aspbs.com/jbn

Hydrolyzed Galactomannan-Modified Nanoparticles and Flower-Like Polymeric Micelles for the Active Targeting of Rifampicin to Macrophages

Marcela A. Moretton[1,2], Diego A. Chiappetta[1,2], Fernanda Andrade[3], José das Neves[3,4], Domingos Ferreira[3], Bruno Sarmento[3,4,5], and Alejandro Sosnik[1,2,*]

[1] *The Group of Biomaterials and Nanotechnology for Improved Medicines (BIONIMED), Department of Pharmaceutical Technology, Faculty of Pharmacy and Biochemistry, University of Buenos Aires, Argentina*
[2] *National Science Research Council (CONICET), Argentina*
[3] *Laboratory of Pharmaceutical Technology, LTF/CICF, Faculty of Pharmacy, University of Porto, Portugal*
[4] *Health Sciences Research Center (CICS), Department of Pharmaceutical Sciences, Instituto Superior de Ciências da Saúde-Norte, Gandra, Portugal*
[5] *INEB – Institute of Biomedical Engineering, University of Porto, Portugal*

Inhalable nanocarriers that are uptaken by macrophages represent an appealing approach for the targeting of antibiotics to the tuberculosis reservoir. In the present work, we report on the development of rifampicin (RIF)-loaded nanoparticles and flower-like polymeric micelles surface-modified with hydrolyzed galatomannan (GalM-h), a polysaccharide of mannose and galactose, two sugars that are recognized by lectin-like receptors. Initially, pure or GalM-h-associated chitosan nanoparticles (NPs) were produced by ionotropic gelation. Despite the composition, NPs displayed positive zeta potential values between +18.0 and +24.5 mV and a size ranging between 263 and 340 nm. In addition, RIF payloads were approximately 1.0% w/w. To increase the encapsulation efficiency, a more complex nanocarrier based on poly(ε-caprolactone)-*b*-poly(ethylene-glycol)-*b*-poly(ε-caprolactone) flower-like polymeric micelles (PMs) coated with chitosan or GalM-h/chitosan were engineered. These polymeric micelles displayed a bimodal size distribution with a positive zeta potential between +6.7 and +8.1 mV. More importantly, the drug encapsulation capacity was increased 12.9-fold with respect to the NPs. An agglutination assay with concanavalin A confirmed the presence of GalM-h on the surface. Qualitative uptake studies by fluorescence microscopy revealed that GalM-h-modified systems were taken-up by RAW 264.7 murine macrophages. Finally, the intracellular/cell associated levels of RIF following the incubation of cells with free or encapsulated drug indicated that while chitosan hinders the uptake, GalM-h leads to a significant increase of the intracellular concentration.

KEYWORDS: *Tuberculosis, Chitosan Nanoparticles, Flower-Like Polymeric Micelles, Hydrolyzed Galactomannan, Rifampicin, Active Drug Targeting to Macrophages.*

INTRODUCTION

Tuberculosis (TB) is the second most lethal infection just behind the human immunodeficiency virus (HIV/AIDS), accounting for approximately 1.5 million annual deaths.[1–4] TB is regarded as a poverty-related disease because it is endemic in developing countries.[5] The World Health Organization (WHO) declared the global sanitary emergency in 1993 owing to the high prevalence of the HIV/TB co-infection.[6] The first-line pharmacotherapy of non-drug resistant TB is divided into two phases combining four drugs and lasting at least six months.[7–9] Both phases comprise the co-administration of rifampicin (RIF) and isoniazid (INH). Regular TB is curable but it still represents more than one quarter of the preventable deaths worldwide[10] and 2.4% of all deaths in the world.[11]

The reduced market profitability of anti-TB drugs and drug delivery systems (DDS) accounts for the relatively

*Author to whom correspondence should be addressed.
E-mail: alesosnik@gmail.com
Received: 17 September 2012
Revised/Accepted: 14 December 2012

slow pace in drug discovery and pharmaceutical product development.[12] On one hand, novel drugs are expected to be more effective against resistant strains than the first-line ones and to shorten the course of the treatment. On the other, they are substantially more expensive and less affordable for patients living in the developing countries mainly hit by the scourge. In this context, the development of innovative nanotechnology-based DDS of first-line drugs that overcome the most relevant biopharmaceutic drawbacks could also lead to a breakthrough in TB pharmacotherapy.[13]

The respiratory system is the primary infection site and the alveolar macrophage (AM) is the cellular reservoir of the non-replicant form of *M. tuberculosis*.[14] Thus, the localized delivery of antibiotics to the lung by the inhalatory route has emerged as an attractive therapeutic approach to reduce the systemic adverse effects associated with the prolonged TB treatment, to prevent hepatic first-pass and to increase the bioavailability of anti-TB drugs in the reservoir.[14, 15] Macrophages can recognize and bind surface mannose residues present in pathogens through specific transmembrane receptors called lectin-like receptors (LLRs). Therefore, the modification of drug nanocarriers with mannose residues has been extensively explored to actively target drugs to LLR-expressing cells.[16–21]

Chitosan (Chit) is a natural polycationic polysaccharide comprising N-acetylglucosamine and glucosamine repeating units[22] (Fig. 1(A)). Due to its good biocompatibility, biodegradability, muco-adhesiveness and great chemical versatility, Chit has been proposed as a novel biomaterial for the development of innovative DDS for administration by various routes.[23–26] Different methods (e.g., microemulsion, emulsion/solvent diffusion, etc.) have been described for the production of drug-loaded Chit micro and nanoparticles (NPs). Nevertheless, ionotropic gelation with polyanions such as tripolyphosphate (TPP) appears as one of the simplest and most reproducible techniques.[23] In addition, different types of micro and nanocarriers have been coated with Chit to attain features such as muco-adhesiveness.[27–30] RIF is one of the most effective anti-TB drugs,[8, 31] though its oral bioavailability is significantly compromised in the presence of INH.[32, 33] At the same time, RIF is an amphiphilic and amphoteric molecule that displays a pH-dependent aqueous solubility (1–3 mg/mL between pH 3–7.4) (Fig. 1(B)). These features challenge the nanoencapsulation of relatively high RIF payloads. In a previous work, we tailored poly(epsilon-caprolactone)-*b*-poly(ethylene glycol)-*b*-poly(epsilon-caprolactone) (PCL-PEG-PCL) "flower-like" polymeric micelles (PMs) for the efficient encapsulation of RIF.[34] The aqueous solubility of the drug was increased from 2.6 to 14.0 mg/mL. This platform is being explored for the development of a liquid RIF/INH fixed dose combination with improved chemical stability and greater oral bioavailability in the treatment of pediatric TB.

Aiming to fine tune the features of this nanotechnology platform to enable the active targeting of antimicrobials to the TB reservoir, in the present study, we report on the development of RIF-loaded flower-like PMs which have been surface-decorated with Chit and hydrolyzed galactomannan (GalM-h) by a solvent diffusion method. GalM is a polysaccharide consisting of a mannose backbone with pendant galactose residues (Fig. 1(C)),[35] both monosaccharides being substrates of LLRs in macrophages. To support the advantageous features of this novel nano-DDS over more conventional ones, their performance in terms of RIF encapsulation capacity and *in vitro* targeting to murine macrophages was compared to that of Chit-NP and Chit/GalM-h-NP produced by a modified ionotropic technique.

MATERIALS AND METHODS

Materials

Epsilon-caprolactone (CL), tin(II) 2-ethylhexanoate (SnOct), chitosan (Chit, low molar mass = ~50 g/mol, deacetylation degree 85%), tripolyphosphate pentasodium salt (TPP), fluorescein 5(6)-isothiocyanate (FITC), bovine serum albumin (BSA), concanavalin A (Con A, from *Canavalia ensiformis*, Jack Bean Type VI) and galactomannan (GalM, locust bean gum from *Ceratonia siliqua* seeds, molar mass = ~310,000 g/mol) were purchased from Sigma-Aldrich (St. Louis, MO, USA). Poly(ethylene glycol) (molar mass = 10,000 g/mol, PEG10000) was supplied by Merck Chemicals (Buenos Aires, Argentina) and dried under vacuum (100–120 °C in an oil bath for 2 h) before use. RIF was purchased from Parafarm® (Buenos Aires, Argentina). Solvents were of analytical or chromatographic grade and were used as received.

Preparation of FITC-Labeled Chitosan

FITC-labeled Chit was obtained as previously described.[36] Briefly, Chit (100 mg) was dissolved in acetic acid (10 mL, final concentration 1.0% w/v) under magnetic stirring. Then, methanol (10 mL) was added to the Chit solution and the mixture was filtered under vacuum. Separately, FITC was dissolved in methanol (2.0 mg/mL) and 10 mL of this solution was incorporated into the Chit filtrate. The mixture was stirred for 3 h protected from light and at room temperature. Then, NaOH 1 M was added dropwise to precipitate the FITC-Chit. Samples were centrifuged and washed with methanol until FITC was visually undetectable in the supernatant. Finally, the obtained FITC-Chit was lyophilized and stored at 4 °C protected from light until use.

Galactomannan Hydrolysis and Characterization

To obtain low molar mass derivatives (GalM-h) displaying greater aqueous solubility and smaller viscosity, GalM was hydrolyzed using trifluoroacetic acid (TFA). Briefly, GalM (1 g) was dispersed in TFA 1 M (40 mL) and

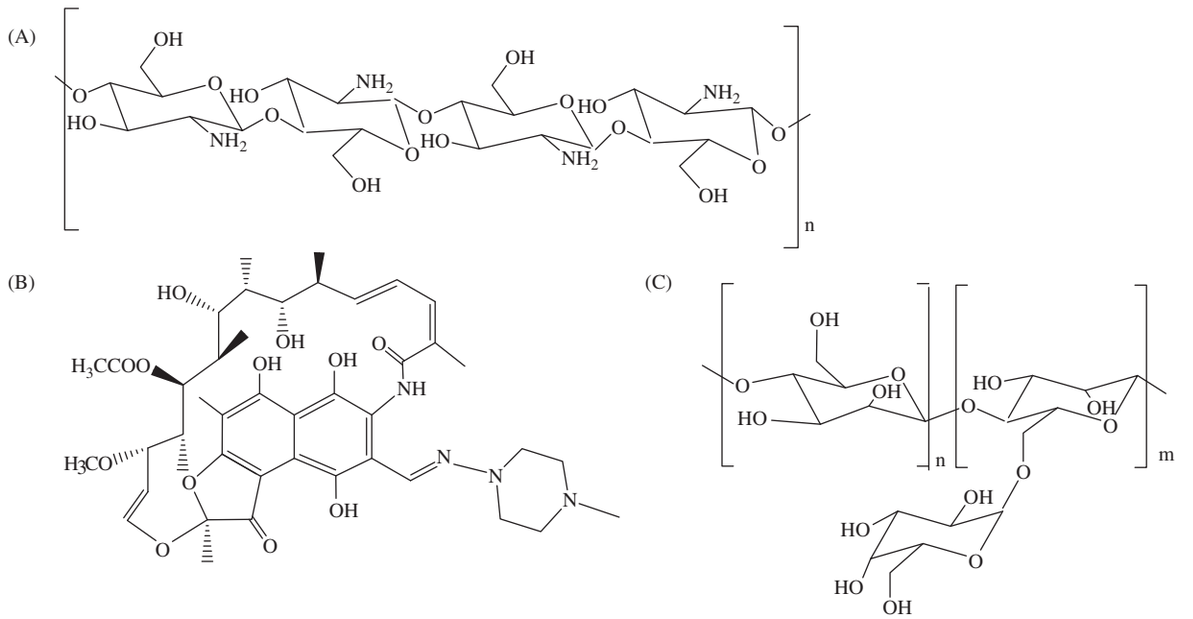

Figure 1. **Chemical structure of (A) chitosan, (B) rifampicin and (C) galactomannan.**

heated at 80 °C for 1 h under magnetic stirring (100 rpm). Then, the mixture was dialyzed (regenerated cellulose dialysis membranes; molecular weight cut off of 3500 g/mol; Spectra/Por® 3 nominal flat width of 45 mm, diameter of 29 mm and volume/length ratio of 6.4 mL/cm; Spectrum Laboratories, Inc., Rancho Dominguez, CA, USA) against distilled water for 24 h and filtered (Whatman® Filter Paper, Grade 91, 10 μm, Piscataway, NJ, USA). Finally, GalM-h was lyophilized (freeze-dryer FIC-L05, FIC, Scientific Instrumental Manufacturing, Argentina; freeze-dryer shelf temperature −14 °C; condenser temperature −40 °C) for 48 h and stored at −20 °C until use. To estimate the viscosity average molar mass (M_v) of GalM-h, the intrinsic viscosity $[\eta]$ was determined applying the Mark-Houwink equation[37]

$$[\eta] = K_h \cdot M_v^{\alpha} \quad (1)$$

Where, K_h is the Mark-Houwink constant related to the polymer chain flexibility and the exponent α represents the chain geometry. In the present study, the values of K_h and α were 3.72×10^{-4} dL/g and 0.74, respectively.[37] The value of $[\eta]$ was determined by measuring the viscosity of diluted GalM-h solutions (concentration between 0.05 and 0.5% w/v) and then extrapolating to an infinite dilution according to the Huggins relationship (2)[38]

$$n_{sp}/c_p = [\eta] + K_h \cdot [\eta]^2 \cdot c_p \quad (2)$$

Where, η_{sp} is the specific viscosity $(\eta_r - 1)$ and C_p is the polysaccharide concentration (g/dL), the η_r value corresponding to the relative viscosity defined as the ratio between the viscosity of the polysaccharide solution and the solvent. The viscosity of diluted GalM-h solutions was determined by a capillary viscometer (Ubbelohde Viscometer Size 1, conversion factor 0.01, kinematic viscosity range 2 to 10 cSt, IVA, Buenos Aires, Argentina) at 25 °C ± 0.1.

Synthesis of PCL-b-PEG-b-PCL Block Copolymer

A PCL-*b*-PEG-*b*-PCL copolymer displaying a central block of PEG10000 and two PCL arms of molar mass 4500 g/mol (PCL4500-PEG10000-PCL4500; $M_{nGPC} = 16,000$ g/mol, $M_{wGPC} = 19,000$ g/mol) was synthesized by the microwave-assisted ring opening polymerization of CL initiated by PEG10000 in the presence of SnOct as described elsewhere.[34] Briefly, dry PEG10000 was mixed with CL (10% molar excess) and SnOct (1/40 molar ratio to CL) in a round-bottom flask, placed in a microwave oven (Itedo™, Japan, radiation frequency 2.45 GHz, maximum operating power 800 W) and the reaction irradiated for 15 min. The crude was dissolved in dichloromethane (50 mL) and precipitated in petroleum ether 35–65 °C (500 mL). This process was repeated one more time to ensure the elimination of monomer and catalyst residues. The white solid product was isolated by filtration, dried at room temperature and stored at −20 °C.

Preparation of PCL4500-PEG10000-PCL4500 Polymeric Micelles Modified with Chit and GalM-h/Chit

Pristine (unmodified) RIF-loaded 1% PMs were prepared following a solvent diffusion technique previously described by our group.[34] For surface-modification with Chit and GalM-h, the preparation technique was slightly modified. Briefly, RIF (50 mg) and PCL4500-PEG10000-PCL4500 (130 mg) were dissolved in acetone

(7 mL) and poured dropwise into an acetic aqueous phase (AcH, 13 mL, final pH of 5.0) using a programmable syringe infusion pump (PC11UB, Apema, Buenos Aires, Argentina) under mechanical stirring (670 rpm, four-blade propeller, IKA® Eurostar Digital Electronic Laboratory Stirrer, IKA®-Werke GmbH & Co. KG, Staufen, Germany) over 20 minutes. To produce 1% PMs coated with Chit (Chit-PM) or a blend of GalM-h and Chit (GalM-h/Chit-PM), Chit (0.1% w/v) or Chit (0.1% w/v)/GalM-h (0.1% w/v) were incorporated into the AcH, respectively. Chit (20 mg) was dissolved in AcH (2.0% v/v, 15 mL, pH 2.7) under mechanical stirring (100 rpm) for 30 min and the pH was adjusted to 5.0 with NaOH 1 M to prevent the acid degradation of RIF.[39] Afterwards, the solution was diluted to a final volume of 20 mL with distilled water (Chit final concentration of 0.2% w/v). For GalM-h/Chit solutions, GalM-h (20 mg) was dissolved in the Chit acetic solution (20 mL, pH 5.0, final concentration of 0.1% w/v). Then, the mixture was stirred for 2 h to ensure complete homogenization of the polysaccharides and filtered (1.2 μm cellulose nitrate membranes, Whatman GmbH, Dassel, Germany) to remove any solid residue. In the case of PMs coated with FITC-Chit and GalM-h/FITC-Chit, the procedure was carried out in the absence of light. RIF-free PMs were prepared as described above though without the incorporation of the drug. The RIF payload was quantified by UV ($\lambda = 482$ nm, Cary [1E] UV–Visible Spectrophotometer Varian, Palo Alto, CA, USA), at 25 °C, employing a calibration curve of RIF in dimethylformamide (DMF) covering the range between 12.5 and 50 μg/mL (correlation factor was 0.9998–0.9999).[40–43] Aliquots (100 μL) were diluted with DMF and filtered (Whatman® Filter Paper, Grade 91, 10 μm). Attempts to replace DMF by a more biocompatible solvent failed. Assays were carried out in triplicate. The RIF loading capacity (LC, expressed in % w/w) was calculated based on the RIF aqueous intrinsic solubility in water (2.56 mg/mL, pH 5.8)[34] according to equation 3

$$\%\text{LC} = (\text{RIF}_T\text{–RIF}_I)/\text{polymer weight} \times 100 \qquad (3)$$

Where, RIF_T and RIF_I are the total amount of RIF in the system and the RIF intrinsic solubility, respectively.

Preparation of RIF-Loaded Chit NPs Modified with GalM-h

Pure Chit NPs (Chit-NP) were prepared by an adapted ionotropic gelation method.[23] In the case of RIF-free systems, Chit (200 mg) was dissolved in AcH (2.0% v/v, 90 mL, pH 2.7) as described above and the pH of the solution was adjusted to 5.0 with NaOH 1 M (Chit final concentration of 0.2% w/v). Then, TPP solution (0.1% w/v, pH of 5.0 adjusted with acetic acid 2.0% v/v) was added dropwise to the Chit solution under magnetic stirring (100 rpm, Chit:TPP molar weight ratio of 6:1, final Chit concentration 0.15% w/v). Afterwards, the mixture was maintained under magnetic stirring for additional 30 min and filtered (Whatman® Filter Paper, Grade 91, 10 μm, Piscataway, NJ, USA). For GalM-h/Chit blend NPs (GalM-h/Chit-NP), GalM-h (0.2% w/v) was added to the Chit solution as described above (GalM-h final concentration of 0.15% w/v). For RIF-loaded Chit-NP and GalM-h/Chit-NP, the drug (0.15 mg/mL) was dissolved in Chit or GalM-h/Chit solution (pH 5.0) and the procedure was followed as described for RIF-free NPs. In the case of FITC-Chit-NP and GalM-h/FITC-Chit-NP, the procedure was carried out protected from light. Samples were centrifuged (20,000 g, refrigerated centrifuge Heraeus Megafuge 1.0 R, Heraeus Centrifuges, Buckinghamshire, UK) for 30 min and the RIF LC (% w/w) was determined according to equation (4)

$$\%\text{LC} = (\text{RIF}_T\text{–RIF}_F)/\text{polymer weight} \times 100 \qquad (4)$$

Where, RIF_T and RIF_F are the total amount of RIF in the suspension before and after centrifugation, respectively. Supernatant aliquots (500 μL) were collected and the RIF concentration was determined by high performance liquid chromatography (HPLC-UV, see below). The choice of an HPLC-UV method at this point relied on the low amount of RIF in supernatants obtained after the production and the centrifugation of the NPs. Also, TPP interfered with UV-Vis detection, leading to non-reproducible baseline data when assessing blank NPs (without RIF) by UV spectrophotometry. The same procedure was followed for RIF-loaded Chit-NP without the addition of GalM-h. RIF solutions were used as controls. All the experiments were carried out in triplicate.

Determination of Size, Size Distribution and Zeta Potential

The hydrodynamic diameter (D_h) and size distribution (polydispersity index, PDI) of the different RIF-free and RIF-loaded nanocarriers were measured by dynamic light scattering (DLS, Zetasizer Nano-Zs, Malvern Instruments, Worcestershire, UK) provided with a 4 mWHe–Ne (633 nm) laser and a digital correlator ZEN3600, at 25 °C. Measurements were conducted at a scattering angle $\theta = 173°$ to the incident beam. Zeta-potential (Z-potential) was determined employing the same equipment. Data are expressed as the average of at least five measurements. Statistical analysis of D_h, PDI and Z-potential was performed by one-way ANOVA test.

Agglutination with Con A

RIF-free nanocarrier dispersions were obtained as described above with a minor modification of the final pH to fit the optimal conditions for Con A tetramerization. In the case of GalM-h/Chit-NP, the pH of TPP 0.1% w/v and Chit 0.2% w/v was adjusted to 6.0 with acetic acid 2.0% v/v and NaOH 1 M, respectively. For Chit-PM and GalM-h/Chit-PM, the pH of AcH was adjusted to the same value

with NaOH 1M. Chit-NP and GalM-h/Chit-NP dispersions were diluted (1/5) with acetate buffer solution (pH 6.0) to prevent BSA precipitation.[44] BSA (90 mg) was added to the different dispersions (2 mL) and the final volume was adjusted to 3 mL with acetate buffer solution (pH 6.0) to obtain a final BSA concentration of 3.0% w/v. Then, samples were incubated at 25 °C for 30 minutes, diluted (1:1) with Con A acetate buffer solution (pH 6.0, 10 μM) and magnetically stirred for 2 and 24 h at room temperature (final concentration of Con A and BSA were 5 μM and 1.5% w/v, respectively). Finally, D_h and PDI were determined by DLS (see above), at 37 °C.

Cell Culture

RAW 264.7 murine macrophage cells (ATCC, Manassas, VA, USA) were maintained in Dulbecco's Modified Eagle's Medium (DMEM) with GlutaMAX™-I (Invitrogen Corporation, Carlsbad, CA, USA) supplemented with fetal bovine serum (10%) and penicillin-streptomycin (final concentration of 10,000 U/ml in penicillin and 10,000 μg/ml in streptomycin, Invitrogen)[36] in a humidified incubator (37 °C, 5% CO_2, Heraeus HERAcell CO_2 incubator, Thermo Scientific, Madison, WI, USA). Cells were detached using a rubber cell scrapper, viability checked by the trypan blue exclusion test and sub-cultured every 3–4 days.

Fluorescence Microscopy

Qualitative cellular uptake of RIF-free FITC-Chit-NP, GalM-h/FITC-Chit-NP and GalM-h/FITC-Chit-PM by RAW 264.7 cells was assessed by fluorescence microscopy. Nanocarriers were dispersed in 2 mL of complete medium (FITC-Chit final concentration = 0.10 mg/mL) and incubated with cells (200,000 cells/well, 37 °C, 5% CO_2) for 1 h. After incubation, cells were washed twice with phosphate buffer solution (PBS, pH 7.4, 2 mL) and DNA was stained with Hoechst 33342 dye (1 μg in 1 mL of medium, Invitrogen Corporation) for 10 min (37 °C, 5% CO_2). Then, cells were washed twice with PBS pH 7.4 (2 mL). For blanks, nanocarrier dispersions without FITC were assayed. Cell viability during the experiments was assessed by performing a trypan blue exclusion test.[53] All the treatments were performed in triplicate. Intracellular uptake was evaluated using a Nikon Eclipse TE 2000 U inverted fluorescence microscope equipped with a digital camera and controlled through Nikon ACT-1 software (Nikon Instruments Inc., Melville, NY, USA).

Quantitative Cellular Uptake of RIF

RAW 264.7 cell suspension (2 mL) was added to each well of a 6-well plate to yield 200,000 cells/well. Afterwards, each plate was incubated (37 °C, 5% CO_2) for 24 h to allow cell attachment. The uptake assays were performed by sucking out the culture medium and washing the cells with PBS (1 × 1 mL, pH 7.4) to remove unattached cells and cellular debris. RIF-loaded systems prepared in culture medium (2 mL) were added to each well (final RIF concentration = 50 μg/mL; 100 μg/well) and incubated for 15, 30, 60, 120, 240 and 360 min (37 °C, 5% CO_2). For every time point, the RIF-loaded dispersion was removed from each well and macrophages were washed twice with PBS pH 7.4 (1 mL). Four-hundred μL of a lysis buffer comprising 10 mM Tris–HCl pH 7.4, 2 mM EDTA pH 8.0, 150 mM NaCl, 0.876% w/v Brij® 97, 0.125% w/v Tween® 20, and one tablet per 50 mL of protease inhibitor cocktail (complete, Mini, EDTA-free; Roche Diagnostics, Indianapolis, IN, USA) was added to each well and the plate was stored at 4 °C for 30 min with sporadic hand-shaking.[49] Cell lysates were collected and centrifuged (13,000 rpm, 10 min, 4 °C). The supernatant was collected and 25 μL was used to assay soluble protein content with a colorimetric-based commercial kit (Pierce® BCA Protein Assay Kit, Thermo Scientific, Rockford, IL, USA). Then, 200 μL of the remaining supernatant was mixed with acetonitrile (400 μL) to precipitate proteins and samples were re-centrifuged (13,000 rpm, 10 min, 4 °C). Finally, the supernatant was collected and the RIF concentration was quantified by HPLC-UV (see below). Results were expressed as the amount of RIF per soluble protein content. Statistical analysis of intracellular/cell associated RIF levels as delivered by the different nanocarriers and the free drug solution for every time point was performed by one-way ANOVA test and Tukey's post-hoc.

HPLC-UV Analysis

The HPLC-UV method was adapted from a method previously described.[54] Briefly, the method consisted of a Dionex UltiMate 3000 LC system (Dionex Corporation, Sunnyvale, CA, USA) with an Xterra® RP18 column (5 μm, 4.6 × 150 mm, Waters Corp., Milford, MA, USA) and mobile phase of acetonitrile:TFA 0.1% (60:40) with a flow rate of 1 ml/min. The injection volume was 20 μL and the linearity range was between 0.05 μg/mL and 5 μg/mL ($R^2 > 0.9998$). The detection was performed at a wavelength of 254 nm and the total elution time was 12 min.

RESULTS AND DISCUSSION

Production and Characterization of RIF-Loaded Nanocarriers

Different NPs and PMs were produced and their size, size distribution and Z-potential were characterized. RIF-free and RIF-loaded Chit-NP displayed a size of 275 and 263 nm, respectively, with a monomodal size distribution and a relatively small PDI value (Table I). These results indicated that the encapsulation of RIF did not alter the size of the NPs, probably due to the relatively low LC of 1.0 ± 0.2% w/w. *Z*-potential values were +23.8 and +24.5 mV owing to the presence of protonated amine groups of Chit on the surface of the NPs. The incorporation of GalM-h to the NPs was aimed to enable the

Table I. RIF payload and size (D_h), size distribution (PDI) and Z-potential values of NPs and PMs at 25 °C ($n = 3$).

Sample	RIF cargo	LC (% w/w) (±S.D.)	D_h (nm) (±S.D.)	PDI (±S.D.)	Z-potential (mV) (±S.D.)
Chit-NP[a]	—	—	275.0 (7.0)	0.28 (0.01)	+23.8 (0.4)
	+	1.0 (0.2)	263.0 (2.0)	0.39 (0.06)	+24.5 (1.0)
GalM-h/Chit-NP[b]	—	—	340.1 (24.0)	0.23 (0.01)	+18.8 (2.1)
	+	1.0 (0.2)	334.4 (26.8)	0.22 (0.01)	+18.0 (0.2)
Chit-PM[c]	—	—	333.9 (15.3)	0.38 (0.06)	+8.1 (0.4)
	+	12.1 (0.3)	239.2* (15.3)	0.41 (0.06)	+6.7 (0.7)
GalM-h/Chit-PM[d]	—	—	344.8 (28.0)	0.47 (0.01)	+8.3 (0.3)
	+	12.9 (0.5)	198.7* (11.0)	0.39 (0.01)	+7.1* (0.3)

[a]Concentration of 0.15%w/v for Chit.
[b]Concentration of 0.15%w/v and 0.15%w/v for Chit and GalM-h, respectively.
[c,d]PMs coated with Chit (0.1 %w/v) or GalM-h/ Chit (0.1 %w/v)/(0.1 %w/v), respectively.
*The size and the Z-potential of RIF-loaded PMs was significantly smaller than that of the RIF-free counterpart ($P < 0.05$).

active targeting of macrophages. At the same time, it was expected to consolidate the structure of the NP polymeric matrix mainly by the generation of hydrogen bonds between both polysaccharide chains[47] and, by doing so, to enhance the RIF encapsulation efficiency. Even though other interactions have been suggested, these appear as the most prominent.[47] GalM-h/Chit-NP were substantially larger than pure Chit ones, sizes being 334 and 340 nm for the drug-free and drug-loaded NPs, respectively. This size increase could be probably associated with the spanning of GalM-h chains of relatively small molar mass on the surface of the NPs; GalM-h showed a M_v of 17.782 g/mol. Z-potential measurements of GalM-h/Chit-NP showed a moderate decrease from +23.8 and +24.5 mV in RIF-free and RIF-loaded Chit-NP to +18.0 and +18.8 mV, strongly suggesting that the incorporation of the neutral GalM-h and its spanning at the surface of the NPs.[44] Moreover, it is worth stressing that GalM-h/Chit-NP maintained their electropositive character that is crucial for muco-adhesiveness. On the other hand, this modification did not improve the LC, the value being also $1.0 \pm 0.2\%$ w/w (Table I). Finally, positively-charged NPs were physically stable over time.

To improve the RIF encapsulation capacity shown by Chit-NP and Chit/GalM-h-NP and, at the same time, to capitalize on the muco-adhesiveness and cell-targeting properties of Chit and GalM-h, respectively, we developed a hybrid nanocarrier: flower-like PCL-*b*-PEG-*b*-PCL PMs surface-decorated with Chit or GalM-h/Chit. Initially, we intended the production employing Chit concentrations of 0.2% and 0.5%, though solutions were too viscous and Chit precipitated upon addition of acetone solution. Thus, the concentration was reduced to 0.1%. To maintain the content of Chit and GalM-h in the micelles similar, the Chit:GalM-h weight ratio was approxiamtely 1:1. This type of PMs is produced by the self-assembly of a block copolymer combining two terminal PCL hydrophobic blocks with a central PEG hydrophilic one and they display a relatively large hydrophobic PCL core that, as we previously reported, enabled the efficient encapsulation of RIF;[34,49] PMs displaying smaller core (e.g., Pluronic) did not effectively encapsulated RIF and formed adducts that decreased the solubility of RIF to values below the intrinsic solubility (unpublished data). Previous reports on the production of PCL NPs coated with Chit by the acetone displacement method indicated that this polysaccharide would be accommodated at the surface.[54] RIF-free Chit-PM and GalM-h/Chit-PM showed D_h values of 334 and 345 nm, respectively, and a monomodal size distribution with PDI of 0.38 and 0.47. These data indicated that the incorporation of Chit and GalM-h led to a sharp increase of the size with respect to 1% RIF-free unmodified PCL4500-PEG10000-PCL4500 PMs that showed D_h of 90 nm.[34] As expected, RIF-loaded Chit-PM and GalM-h/Chit-PM remained larger than their respective unmodified counterpart[34] though they were substantially smaller than RIF-free Chit-PM and Chit/GalM-h-PM, sizes being 239 and 199 nm, respectively (Table I). Conversely, PDI values remained almost unchanged. These findings would stem from the modified self-aggregation pattern of PCL4500-PEG10000-PCL4500 in presence of RIF.[34] Since the NP counterparts are not self-assembly systems and their size was not altered upon drug encapsulation. Modified PMs showed the low physical stability that is characteristic of PCL-*b*-PEG-*b*-PCL polymeric micelles. To prevent micellar re-aggregation a freeze- or spray drying process should be required; the latter being more convenient for scale-up. This study was beyind the goal of the work and it will be assessed in the future.

Z-potential analysis of Chit-PM and Chit/GalM-h-PM showed positive values between +6.7 and +8.3 mV. A decrease in the Z-potential value of PMs with respect to Chit-NP and Chi/GalM-h-NP suggested that the positively charged Chit was less available in the surface of PMs than in that of NPs, probably due to a lower Chit absolute concentration in the nanocarrier. An additional phenomenon could be the shielding effect of PEG blocks of the amphphilic copolymer. In any event, positive Z-potential confirmed that Chit was available in the surface. Otherwise,

the zeta potential would be almost neutral as in the unmodified micelles.[34] Unlike GalM-h/Chit-NP, the incorporation of GalM-h to Chit-PM did not substantially alter the *Z*-potential with respect to Chit-PM (Table I), indicating that positively-charged Chit chains were not shielded by GalM-h and that they were still available in the surface of the micelles.

Drug encapsulation studies showed encouraging results with LC values as high as $12.9 \pm 0.5\%$ w/w, this level representing an almost 13 times increase in the drug payload with respect to the different NPs under investigation that yielded RIF cargos of approximately 1%. This solubility increase could be related to the great hydrophobicity of the micellar core with respect to the water-rich hydrophilic polymeric matrix of Chit-NP and Chit/GalM-h-NP that was conveniently tailored to display a size that enables the hosting of bulky RIF molecules.[34]

Agglutination with Con A

Aiming to assess the availability of mannose residues at the surface of the nanocarriers and the efficiency of the recognition by carbohydrate-binding lectins (e.g., LLRs), samples were incubated with a soluble lectin and the size was monitored by DLS.[51] Con A is a globular protein that exhibits a tetrameric form above pH 7 and a dimeric form below pH 5. Between these pH values, both forms have been found to co-exist.[52] In this work, the final pH value of the dispersions was adjusted to 6.0 in order to prevent Chit precipitation (pK_a value for Chit amine groups is ~6.5).[23] Con A has been widely used in the study of glycoproteins, glycopeptides and cell structures as it selectively binds to α-D-mannosyl and α-D-glucosyl residues.[53] It is important to remark that only the tetramer exhibits four independent sugar binding sites[54] and the ability to generate large aggregates due the interaction with several sugar residues. For an optimal binding, tetrameric Con A demands the presence of Ca^{2+} ions and the availability of unmodified hydroxyl groups at positions C-3, C-4 and C-6 in the pyranose ring.[55, 56] On the other hand, previous studies demonstrated the weak, though effective, interaction of a secondary binding site in Con A with the gluconic acid residue of lactobionic acid.[57–59] In this study, BSA was added as Ca^{2+} supplement.[51] Results of size and size distribution before and after incubation with Con A are presented in Table II. BSA presented a unimodal size distribution with a peak of 19 nm, while BSA/Con A mixture a bimodal one. The minor small-size population (14 nm) corresponded to BSA and the large-size one (221 nm) to BSA/Con A aggregates (Table II). It is worth mentioning that the BSA size distribution is strongly affected by the protein concentration and properties of the medium such as pH. The D_h measured in this study was slightly larger than the main population that we previoulsy measured at pH 7.4 though, in that work also observed a large-size population of up to 200 nm.[60] After 24 h, a monomodal size pattern (547 nm) was observed, indicating the progressive inespecific co-aggregation of both proteins. When a GalM-h solution was incubated with BSA/Con A, the size pattern was similar to that of BSA/Con A solution with a slight

Table II. Size and size distribution of Chit-NP, GalM-h/Chit-NP, Chit-PM and GalM-h/Chit-PM before and after addition of Con A. All the samples were added BSA ($n = 3$).

			D_h (nm) (±S.D.)						
Sample	Time (h)	Con A	Peak 1	% Intensity	Peak 2	% Intensity	Peak 3	% Intensity	PDI (±S.D.)
BSA control[a]	0	—	19.1 (1.3)	100	—	—	—	—	0.24 (0.01)
BSA/Con A[b]		+	13.8 (2.0)	15.3	221.3 (17.4)	84.7	—	—	0.43 (0.09)
	24	+	547.0 (68.9)	100	—	—	—	—	0.81 (0.15)
GalM-h solution[c]	0	+	12.7 (2.4)	14.0	263.0 (29.7)	86.0	—	—	0.48 (0.06)
	24	+	433.5 (30.0)	100	—	—	—	—	0.94 (0.07)
Chit-NP[d]	0	—	21.0 (3.3)	30.5	246.3 (73.7)	69.5	—	—	0.56 (0.03)
		+	14.3 (1.8)	16.6	225.7 (17.3)	83.4	—	—	0.51 (0.16)
	24	+	11.3 (1.5)	11.3	280.1 (45.5)	88.7	—	—	0.40 (0.06)
GalM-h/Chit-NP[d]	0	—	15.8 (2.2)	67.5	172.5 (43.2)	32.5	—	—	0.47 (0.04)
		+	17.1 (5.3)	14.3	285.1 (19.3)	85.7	—	—	0.66 (0.03)
	24	+	434.7 (120.0)	42.7	1522.5 (34.7)	27.3	4626.0 (316.2)	30.0	1.00 (0.07)
Chit-PM[e]	0	—	51.3 (7.2)	14.1	294.7 (19.3)	81.9	5255.7 (132.2)	3.2	0.62 (0.09)
		+	29.0 (3.7)	9.1	271.6 (22.8)	84.3	5202.7 (359.0)	6.6	0.51 (0.10)
	24	+	14.87 (0.1)	4.1	191.9 (8.7)	88.9	5272.3 (136.2)	7.0	0.55 (0.04)
GalM-h/Chit-PM[e]	0	—	220.0 (1.5)	100.0	—	—	—	—	0.50 (0.01)
		+	214.7 (6.3)	70.1	4172 (35.4)	29.9	—	—	0.71 (0.03)
	24	+	>8 μm	—	—	—	—	—	—

[a] BSA 1.5 % w/v in acetate buffer solution of pH 6.0.
[b] Acetate buffer pH 6.0 + BSA 1.5 %w/v + Con A 5μM.
[c] GalM-h control solution (0.1 %w/v).
[d] NPs dilution (1/5) with acetate buffer pH 6.0.
[e] GalM-h/Chit (0.1/0.1 %w/v) or Chit (0.1 %w/v).

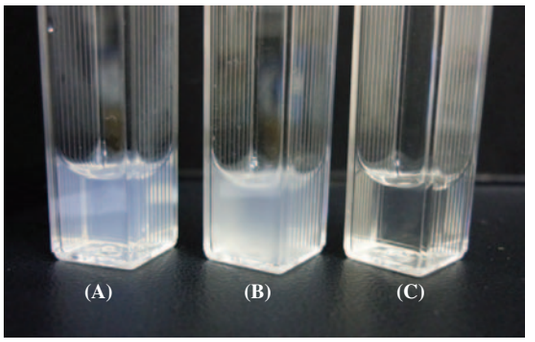

Figure 2. **(A,B) Image of GalM-h/Chit-PM dispersions (A) before and (B) after incubation with Con A 5 μM for 2h. (C) Acetate buffer pH 6.0 with BSA 1.5 % w/v and Con A 5 μM (control solution) after incubation for 2 h.**

size increase of the second population to 263 nm at 2 h and a later size growth to 433 nm at 24 h. Upon the addition of BSA, both Chit-NP and GalM-h/Chit-NP showed a bimodal size distribution. In case of Chit-NP, two size fractions of 21 and 246 nm were consistent with the presence of a mixture of BSA aggregates and NPs (Table II). Despite the incubation time, this pattern did not undergo substantial changes in presence of Con A, this behavior stemming from the absence of GalM-h. GalM-h/Chit-NP behaved different. After the addition of BSA, two size populations of 15 and 172 nm were observed (Table II), indicating no agglutination. Conversely, after incubation with BSA/Con A for 2 h, the major peak grew from 172 to 285 nm and the PDI value from 0.47 to 0.66 (Table II). After 24 h, the size of the aggregates ranged between 434 nm and 4.6 μm, being apparent even to the naked eye (data not shown). These results indicated the further Con A-mediated agglutination of the nanocarriers owing to the presence of GalM-h at the surface. Regardless of the incubation time, the size pattern of Chit-PM in BSA and BSA/Con A was very similar due to the absence of GalM-h (Table II). The presence of a very small size fraction of 5 μm could be probably assigned to some inespecific aggregation. Contrary to this, GalM-h/Chit-PM showed a fast and sharp increase in size from 220 nm up to 4.2 μm even after 2 h (Table II). This result was visualized as an increase in the dispersion turbidity (Fig. 2). Moreover, at 24 h, aggregates were larger than >8 μm. A similar behavior was reported for surface mannosylated liposomes.[53] Overall these results confirmed the advantageous features of PMs that combined a significantly greater RIF encapsulation capacity with mannose residues in the surface for the effective recognition and binding to LLRs.

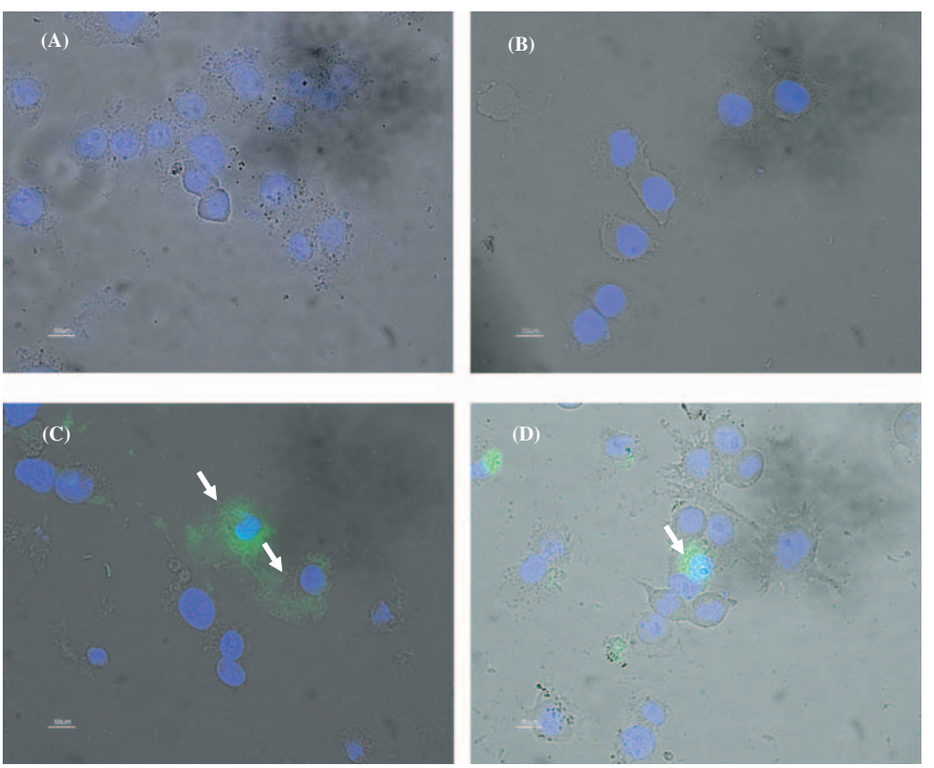

Figure 3. **Fluorescence microscopy images of macrophage cells incubated for 1h with (A) PBS pH 7.4, (B) FITC-Chit-NP (Chit final concentration: 0.1 mg/mL), (C) GalM-h/FITC-Chit-NP (GalM-h/Chit final concentration: 0.1/0.1 mg/mL, respectively) and (D) GalM-h/FITC-Chit-PM (GalM-h/Chit final concentration: 0.1/0.1 mg/ml, respectively). Nuclei are stainned blue with Hoechst 33342. White arrows in C and D show green fluorescence in the macrophage cytosol due to the uptake of GalM-h-containing nanocarriers (Magnification 40x).**

In Vitro Macrophage Uptake

Phagocytosis is an energy-dependent process that requires the primary adhesion of the NP to the cell surface and it represents the main mechanism for active NP uptake by macrophages.[61] Many phagocytosis studies have been performed using microcarriers loaded with different anti-TB drugs.[62–64] Even though macrophages efficiently internalize micron-sized particles but less frequently nano-sized ones,[65] recent studies have confirmed the efficient internalization of retinoic acid-loaded nanospheres and nanocapsules[66, 67] and insulin-loaded solid lipid NPs[36] by macrophages.

To confirm that the modification of the NPs and PMs with GalM-h promotes the uptake by macrophages, the internalization of the different nano-DDS and the intracellular/cell associated RIF levels were assessed in two different experiments. First, the internalization was studied qualitatively by fluorescence microscopy employing FITC-labeled NPs and PMs that were incubated for 1 h with murine macrophages (Fig. 3). A negative control of macrophages incubated with PBS pH 7.4 showed no green fluorescence, indicating the absence of cell background fluorescence that could interfere with fluorescein (Fig. 3(A)). A similar result was obtained with FITC-Chit-NP owing to the absence of mannose targeting moieties (Fig. 3(B)). These data correlated well with the low intracellular/cell associated RIF levels, as assessed in the quantitative studies (Fig. 4). Moreover, for every time point, a significant decrease ($P < 0.05$) in the intracellular/cell associated RIF concnetrations with respect to the free RIF control solution (50 μg/mL) was observed; RIF concentration did not exceed 0.4 μg/mg protein with Chit-NP, while it was greater than 0.55 μg/mg for the RIF-control solution. Furthermore, intracellular/cell associated RIF levels between 15 min and 6 h showed a negligible increase. These results were in accordance with qualitative uptake results and strongly suggested that no active NP internalization took place and that Chit hampered the internalization of RIF. Some authors described that positively-charged particles are more prone to be taken up by phagocytic cells (e.g., macrophages) than negatively-charged ones.[61] However, this characteristic did not improve the internalization of Chit-NP displaying a Z-potential of +24.5 mV (Table I). This phenomenon might be related to the Chit hydrophilic nature which could impart stealth properties that prevent macrophage uptake, as previously reported with Chit-coated loid lipid nanoparticles.[36] In this context, the very slight increase of RIF levels with Chit-NP could be related to the release of drug from the NPs to the culture medium and its subsequent RIF internalization by diffusion owing to a concentration gradient.

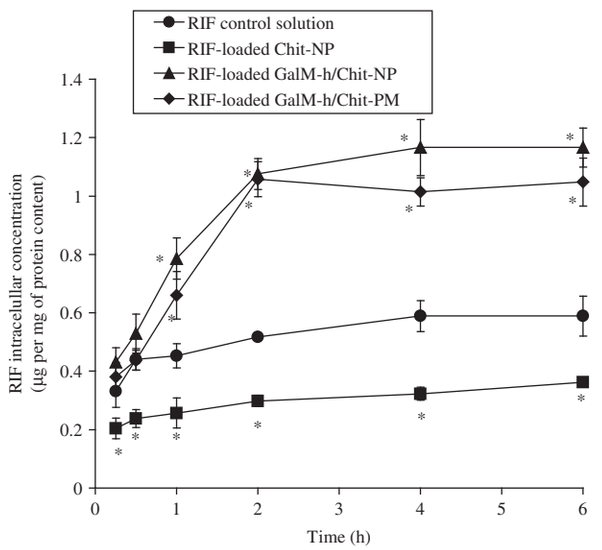

Figure 4. Time-dependent intracellular/cell associated RIF levels in murine macrophages (RAW 264.7) for RIF-loaded Chit-NP, GalM-h/Chit-NP and GalM-h/Chit-PM in comparison with RIF control solutions. The RIF concentration in all the samples was 50 μg/mL. Assays were done in triplicate. $P < 0.05$ indicates a significant increase or decrease of the RIF intracellular levels with respect to free RIF (one-way ANOVA test with Tukey's test post-hoc). The difference between GalM-h/Chit-NP and GalM-h/Chit-PM was not statistically significant at any time point.

To overcome poor cell uptake, the surface of the NPs was modified with mannose residues, a monosaccharide that binds specific receptors expressed by antigen-presenting cells such as macrophages and dendritic cells.[68] In this study, we employed GalM, a natural polysaccharide composed of D-galactose and D-mannan where the latter is a cell wall component of microorganisms consisting in D-mannose residues.[48] Due to its structure, a blend with Chit led to the formation of NPs with superficial mannose residues. After 1 h incubation of GalM-h/FITC-Chit-NP with macrophages, green fluorescence was clearly visualized in the cytosol (Fig. 3(C)). These results suggested the active internalization of the NPs containing GalM-h as opposed to the pure Chit counterpart. Concomitantly, RIF internalization assays showed a pronounced 2-fold increase of the intracellular/cell associated drug concentration to 1.1 μg per mg of protein content between 15 min and 2 h with a less pronounced increment later on (Table III). The increase of the concentration in these time lapse was linear ($R^2 = 0.9824$) (Fig. 4). Moreover, for every time point, the drug intracellular/cell associated level was significantly ($P < 0.05$) greater than with the free RIF solution. These results demonstrated that the incorporation of GalM-h led to a sharp increase of the uptake of RIF-loaded NPs. It has been reported that phagocytosis is very active during the first 4 h and that it gradually decreases afterwards due to saturation.[68] Our results were in good agreement with the literature.

Taking into account the positive effect provided by the addition of GalM-h and the dramatically greater encapsulation capacity of the PMs, RIF-loaded PMs coated with

Table III. RIF intracellular levels ratio between RIF-loaded Chit-NP, GalM-h/Chit-NP or GalM-h/Chit-PM and a free RIF-control solution.

Time (min)	Chit-NP[a]	GalM-h/Chit-NP[b]	GalM-h/Chit-PM[c]
15	0.6	1.3	1.1
30	0.5	1.2	1.0
60	0.6	1.7	1.5
120	0.6	2.1	2.0
240	0.5	2.0	1.7
360	0.6	2.0	1.8

[a]Chit concentration was 0.1 mg/ml.
[b,c]Chit and GalM-h concentration was 0.1 mg/ml.

Chit/GalM-h were also tested in uptake assays. Again, the internalization could be appreciated after incubation of macrophages with GalM-h/FITC-Chit-PM for 1 h as a green fluorescence in the cytosol (Fig. 3(D)). RIF intracellular/cell associated levels were similar to those attained with GalM-h/Chit-NP and significantly higher than with the control (Table III, Fig. 4); also here a lineal RIF internalization profile was achieved during the first 2 h ($R^2 = 0.9968$). Since it was robustly demonstrated that Chit-NP curtails RIF uptake and leads to RIF concentrations that were smaller than a free RIF suspension and dramatically smaller than GalM-h-modified NPs, we did not include Chit-PM in this study.

It should be stressed that the RIF initial concentration was, in all the samples, adjusted to 50 μg/mL by diluting both GalM-h/FITC-Chit-NP and GalM-h/FITC-Chit-PM before the assay. In this framework, the micellar dispersion that contained a substantially greater initial drug concentration (3.85 mg/mL) with respect to the NPs (0.15 mg/mL) was diluted to a much greater extent, leading to samples that contained a significantly smaller amount of RIF-loaded nanocarriers per volume unit. Considering this, GalM-h/Chit-PM would appear as more efficient nano-DDS than GalM-h/Chit-NP for the targeting of RIF to macrophages. On the other hand, *in vivo* assays in an infected animal model would be mandatory to establish the most appropriate and effective nano-DDS and the effective dose.

CONCLUSION

The present study reports on the development of nano-DDS surface-decorated with GalM-h, an oligosaccharide that contains mannose residues recognizable by LLRs, as a strategy effectively encapsulate and actively cell-target RIF to macrophages in the treatment of TB. The interaction of mannose residues of GalM-h with a soluble lectin, Con A, was preliminarly confirmed *in vitro* by DLS. Moreover, assays employing murine macrophages demonstrated that RIF-loaded NPs could not be efficiently taken up without the modification of the surface with GalM-h. To further improve the RIF payload and expand the versatility of the nanocarriers, a novel nano-DDS that capitalized on the high encapsulation capacity of flower-like polymeric micelles and the biopharmaceutic features of Chit and GalM-h were engineered and efficiently produced. These systems not only displayed a dramatic increase of the RIF cargo from 1.0% to 12.9% w/w but they also ensured the active internalization of the drug by macrophages *in vitro*. Future studies will be focused on the development of powders for inhalation, the measurement and fine tuning of the aerodynamic diameter that governs the deposition process in the airways and the *in vitro* release, permeation and cytotoxicity of RIF-loaded GalM-h/Chit-PM.

Acknowledgments: MAM thanks a Ph.D. scholarship of CONICET. DAC and AS are staff-members of CONICET. The authors thank the exchange program between the Ministry of Science, Technology and Innovation (Argentina) and the Fundacao para a Ciencia e Tecnologia (Portugal).

REFERENCES

1. WHO, Global tuberculosis control: Surveillance, planning, financing. World Health Organization: Geneva, Switzerland. http://www.who.int/tb/publications/global_report/2008/pdf/fullreport.pdf **(2008)**, (Accessed July 2010).
2. S. H. Kaufmann and A. J. McMichael, Annulling a dangerous liaison: Vaccination strategies against AIDS and tuberculosis. *Nat. Med.* 11, S33 **(2005)**.
3. T. R. Frieden, T. R. Sterling, S. S. Munsiff, C. J. Watt, and C. Dye, Tuberculosis. *Lancet* 362, 887 **(2003)**.
4. S. Sharma, P. K. Sharma, N. Kumar, and R. Dudhe, A review on various heterocyclic moieties and their antitubercular activity. *Biomed. Pharmacother.* 65, 244 **(2011)**.
5. S. Bertel Squire and S. Thomson, in Tuberculosis-A comprehensive clinical reference, Edited by H. Simon Schaaf, A. L. Zumla, J. M. Grange, M. C. Raviglione, W. W. Yew, J. R. Starke, M. Pai, and P. R. Donald, Saunders Elsevier, London **(2009)**, pp. 908–915.
6. WHO, WHO declares tuberculosis a global emergency. *Soc. Prevent. Med.* 38, 251 **(1993)**.
7. WHO, Treatment of tuberculosis: guidelines, 4th Ed. World Health Organization: Geneva, Switzerland. http://whqlibdoc.who.int/publications/2010/9789241547 833_eng.pdf **(2010)**, (Accessed August 2012).
8. E. C. Rivers and R. L. Mancera, New antituberculosis drugs in clinical trials with novel mechanism of action. *Drug Discov. Today* 13, 1090 **(2008)**.
9. A. Matteelli, A. Carvalho, K. E. Dooley, and A. Kritski, TMC207: The first compound of a new class of potent anti-tuberculosis drugs. *Future Microbiol.* 5, 849 **(2010)**.
10. S. T. Cole, R. Brosch, J. Parkhill, T. Garnier, C. Churcher, D. Harris, S. V. Gordon, K. Eiglmeier, S. Gas, C.E. 3rd. Barry, F. Tekaia, K. Badcock, D. Basham, D. Brown, T. Chillingworth, R. Connor, R. Davies, K. Devlin, T. Feltwell, S. Gentles, N. Hamlin, S. Holroyd, T. Hornsby, K. Jagels, A. Krogh, J. McLean, S. Moule, L. Murphy, K. Oliver, J. Osborne, M. A. Quail, M. A. Rajandream, J. Rogers, S. Rutter, K. Seeger, J. Skelton, R. Squares, S. Squares, J. E. Sulston, K. Taylor, S. Whitehead, and B. G. Barrell, Deciphering the biology of*Mycobacterium tuberculosis* from the complete genome sequence, *Nature* 393, 537 **(1998)**.
11. WHO, The top ten causes of death. World Health Organization: Geneva, Switzerland. http://www.who.int/mediacentre/factsheets/fs310/en/index.html **(2011)** (Accessed August 2012).

12. P. Trouiller, P. Olliaro, E. Torreele, J. Orbinski, R. Laing, and N. Ford, Drug development for neglected diseases: A deficient market and a public-health policy failure. *Lancet* 359, 2188 **(2002)**.

13. A. Sosnik, A. M. Carcaboso, R. J. Glisoni, M. A. Moretton, and D. A. Chiappetta, New old challenges in tuberculosis: Potentially effective nanotechnologies in drug delivery. *Adv. Drug Deliv. Rev.* 62, 547 **(2010)**.

14. R. Pandey and G. K. Khuller, Antitubercular inhaled therapy: Opportunities, progress and challenges. *J. Antimicrob. Chemother.* 55, 430 **(2005)**.

15. F. Andrade, D. Ferreira, A. Sosnik, and B. Sarmento, in Emerging Topics in Nanotechnology, Edited by A. Eftekhari, John Wiley & Sons, New York **(2012)**, in press.

16. Y. Han, L. Zhao, Z. Yu, J. Feng, and Q. Yu, Role of mannose receptor in oligochitosan-mediates stimulation of macrophage function. *Int. Immunopharmacol.* 5, 1533 **(2005)**.

17. H-L. Jiang, M-L. Kang, J-S. Quan, S-G. Kang, T. Akaike, and H. S. Yoo, The potential of mannosylated chitosan microspheres to target macrophage mannose receptors in an adjuvant-delivery system for intranasal immunization. *Biomaterials* 29, 1931 **(2008)**.

18. J. M. Irache, H. H. Salman, C. Gamazo, and S. Espuelas, Mannose-targeted systems for the delivery of therapeutics. *Expert Opin. Drug Deliv.* 5, 703 **(2008)**.

19. E. H. Song, M. J. Manganiello, Y. H. Chow, B. Ghosn, A. J. Convertine, P. S. Stayton, L. M. Schnapp, and D. M. Ratner. *In vivo* targeting of alveolar macrophages via RAFT-based glycopolymers. *Biomaterials* 33, 6889 **(2012)**.

20. R. Duncan, Polymer conjugates as anticancer nanomedicines. *Nat. Rev. Cancer* 6, 688 **(2006)**.

21. M. Alonso-Sande, D. Teijeiro-Osorio, C. Remuñán-López, and M. J. Alonso, Glucomannan, a promising polysaccharide for biopharmaceutical purposes. *Eur. J. Pharm. Biopharm.* 72, 453 **(2009)**.

22. V. K. Mourya and N. N. Inamdar, Chitosan-modifications and applications opportunities galore. *React. Funct. Polym.* 68, 1013 **(2008)**.

23. K. Nagpal, S. K. Singh, and D. N. Mishra, Chitosan nanoparticles: A promising system in novel drug delivery. *Chem. Pharm. Bull.* 58, 1423 **(2010)**.

24. F. Andrade, F. Goycoolea, D. A. Chiappetta, J. das Neves, A. Sosnik, and B. Sarmento, Chitosan-grafted copolymers and chitosan-ligand conjugates as matrices for pulmonary drug delivery. *Int. J. Carbohydr. Chem. Art.* 865704 **(2011)**.

25. A. Nasti, N. M. Zaki, P. de Leonardis, S. Ungphaiboon, P. Sansongsak, M. G. Rimoli, and N. Tirelli, Chitosan/TPP and chitosan/TPP-hyaluronic acid nanoparticles: Systematic optimisation of the preparative process and preliminary biological evaluation. *Pharm. Res.* 26, 1918 **(2009)**.

26. S. Rodrigues, A. M. R. da Costa, and A. Grenha, Chitosan/carrageenan nanoparticles: Effect of cross-linking with tripolyphosphate and charge ratios. *Carbohydr. Polym.* 89, 282 **(2012)**.

27. M. L. Manca, M. Manconi, D. Valenti, F. Lai, G. Loy, P. Matricardi, and A. M. Fadda, Liposomes coated with chitosan–xanthan gum (chitosomes) as potential carriers for pulmonary delivery of rifampicin. *J. Pharm. Sci.* 101, 566 **(2012)**.

28. A. Jayasree, S. Sasidharan, M. Koyakutty, S. Nair, and D. Menon, Mannosylated chitosan-zinc sulphide nanocrystals as fluorescent bioprobes for targeted cancer imaging. *Carbohydr. Polym.* 85, 37 **(2011)**.

29. S. S. Chakravarthi and D. H. Robinson, Enhanced cellular association of paclitaxel delivered in chitosan-PLGA particles. *Int. J. Pharm.* 409, 111 **(2011)**.

30. P. Fonte, T. Nogueira, C. Gehm, D. Ferreira, and B. Sarmento, Chitosan-coated solid lipid nanoparticles enhance the oral absorption of insulin. *DrugDeliv. Transl. Res.* 1, 299 **(2011)**.

31. L. C. du Toit, V. Pillay, and M. P. Danckwerts, Tuberculosis chemotherapy: current drug delivery approaches. *Respir. Res.* 7, 118 **(2006)**.

32. C. J. Shishoo, S. A. Shah, I. S. Rathod, S. S. Savale, J. S. Kotecha, and P. B. Shah, Stability of rifampicin in dissolution medium in presence of isoniazid. *Int. J. Pharm.* 190, 109 **(1999)**.

33. S. Singh, T. T. Mariappan, N. Sharda, S. Kumar, and A. K. Chakrabarti, The reason for an increase in decomposition of rifampicin in the presence of isoniazid under acid conditions. *Pharm. Pharmacol. Comm.* 6, 405 **(2000)**.

34. M. A. Moretton, R. J. Glisoni, D. A. Chiappetta, and A. Sosnik, Molecular implications in the nanoencapsulation of the antituberculosis drug rifampicin within flower-like polymeric micelles. *Colloids Surf. B Biointerfaces* 79, 467 **(2010)**.

35. J. B. Pristov, A. Mitrovic', and I. Spasojevic', A comparative study of antioxidative activities of cell-wall polysaccharides. *Carbohydr. Res.* 346, 2255 **(2011)**.

36. B. Sarmento, D. Mazzaglia, M. C. Bonferoni, A. P. Neto, M. Monteiro, and V. Seabra, Effect of chitosan coating in overcoming the phagocytosis of insulin loaded solid lipid nanoparticles by mononuclear phagocyte system. *Carbohydr. Polym.* 84, 919 **(2011)**.

37. D. R. Picout and S. B. Ross-Murphy, On the Mark–Houwink parameters for galactomannans. *Carbohydr. Polym.* 70, 145 **(2007)**.

38. R. J. Young and P. A. Lovell, Editors, Introduction to polymers, Vol. 2, Chapman & Hall. New York **(1991)**.

39. R. Sankar, N. Sharda, and S. Singh, Behavior of decomposition of rifampicin in the presence of isoniazid in the pH range 1–3. *Drug Dev. Ind. Pharm.* 29, 733–738 **(2003)**.

40. C. J. Shishoo, S. A. Shah, I. S. Rathod, and S. S. Savale, Impared bioavailability of rifampicin from fixed dose combinations (FDC) formulations with isoniazid. *Indian J. Pharm. Sci.* 63, 443 **(2001)**.

41. L. Chen, Z. Xie, J. Hu, X. Chen, and X. Jing, Enantiomeric PLA–PEG block copolymers and their stereocomplex micelles used as rifampin delivery. *J. Nanopart. Res.* 9, 777 **(2007)**.

42. S. K. Mehta, N. Jindal, and G. Kaur, Quantitative investigation, stability and *in vitro* release studies of anti-TB drugs in triton niosomes. *Colloids Surf. B Biointerfaces* 87, 173 **(2011)**.

43. S. K. Mehta and N. Jindal, Formulation of tyloxapol niosomes for encapsulation, stabilization and dissolution of anti-tubercular drugs. *Colloids Surf. B Biointerfaces* 101, 434 **(2013)**.

44. H. Morawetz and W. L. Hughes, The interaction of proteins with synthetic polyelectrolytes I. Complexing of bovine serum albumin. *J. Phys. Chem.* 56, 64 **(1952)**.

45. J. das Neves, J. Michiels, K. K. Ariën, G. Vanham, M. Amiji, M. F. Bahia, and B. Sarmento, Polymeric Nanoparticles Affect the Intracellular Delivery, Antiretroviral Activity and Cytotoxicity of the Microbicide Drug Candidate Dapivirine. *Pharm. Res.* 29, 1468 **(2012)**.

46. I. Calleja, M. J. Blanco-Príeto, N. Ruz, M. J. Renedo, and M. C. Dios-Viéitez, High-performance liquid–chromatographic determination of rifampicin in plasma and tissues. *J. Chromatogr. A* 130, 289 **(2004)**.

47. W. Lin, Q. Li, and T. Zhu, New chitosan/Konjac glucomannan blending membrane for application in pervaporation dehydration of caprolactam solution. *J. Ind. Chem. Eng.* 18, 934 **(2012)**.

48. M. Samil Kök, Rheological study of galactomannan depolymerization at elevated temperatures: Effect of varying pH and addition of antioxidants. *Carbohydr. Polym.* 81, 567 **(2010)**.

49. M. A. Moretton, D. A. Chiappetta, and A. Sosnik, Cryoprotection–lyophilization and physical stabilization of rifampicin loaded flower-like polymeric micelles. *J. Royal Soc. Interface* 9, 487 **(2012)**.

50. L. Mazzarino, C. Travelet, S. Ortega-Murillo, I. Otsuka, I. Pignot-Paintrand, E. Lemos-Senna, and R. Borsali, Elaboration of chitosan-coated nanoparticles loaded with curcumin for mucoadhesive applications. *J. Colloid. InterfaceSci.* 370, 58 **(2012)**.

51. X. Wang, O. Ramström, and M. Yan, Dynamic light scattering as an efficient tool to study glyconanoparticle–lectin interactions. *Analyst* 136, 4174 **(2011)**.

52. J. Bouckaert, R. Loris, and L. Wyns, Zinc/calcium- and cadmium/cadmium-substituted concanavalin A: interplay of metal binding, pH and molecular packing. *Acta Crystallogr. D Biol. Crystallogr.* 56, 1569 **(2000)**.
53. A. Štimac, S. Šegota, M. Dutour Sikirić, R. Ribić, L. Frkanec, V. Svetličić, S. Tomić, B. Vranešić, and R. Frkanec, Surface modified liposomes by mannosylated conjugates anchored via the adamantly moiety in the lipid bilayer. *Biochim. Biophys. Acta* 1818, 2252 **(2012)**.
54. G. Sánchez-Pomales, T. A. Morris, J. B. Falabella, M. J. Tarlov, and R. A. Zangmeister, A lectin-based gold nanoparticle assay for probing glycosylation of glycoproteins. *Biotechnol. Bioeng.* 109, 2240 **(2012)**.
55. Y. Anraku, Y. Takahashi, H. Kitano, and M. Hakari, Recognition of sugars on surface-bound cap-shaped gold particles modified with a polymer brush. *Colloids Surf. B Biointer.* 57, 61 **(2007)**.
56. R. Yin, Z. Tong, D. Yang, and J. Nie, Glucose-responsive insulin delivery microhydrogels from methacrylated dextran/concanavalin A: Preparation and *in vitro* release study. *Carbohydr. Polym.* 89, 117 **(2010)**.
57. M-X. Hu and Z-K. Xu, Carbohydrate decoration of microporous polypropylene membranes for lectin affinity adsorption: Comparison of mono- and disaccharides. *Colloids Surf. B Biointerfaces* 85, 19 **(2011)**.
58. X. Wang, L. H. Liu, O. Ramström, and M. Yan, Engineering nanomaterial surfaces for biomedical applications. *Exp. Biol. Med.* 234, 1128 **(2009)**.
59. Y. H. Choi, F. Liu, J. S. Park, and S. W. Kim, Lactose-poly(ethylene glycol)-grafted poly-L-lysine as hepatoma cell-tapgeted gene carrier. *Bioconjug. Chem.* 9, 708 **(1998)**.
60. D. A. Chiappetta, C. Hocht, J. A. W. Opezzo, and A. Sosnik, Intranasal administration of antiretroviral-loaded micelles for anatomical targeting to the brain in HIV, Nanomedicine (Lond.), in press.
61. T. Onoshita, Y. Shimizu, N. Yamaya, M. Miyazaki, M. Yokoyama, N. Fujiwara, T. Nakajima, K. Makino, H. Terada, and M. Haga, The behavior of PLGA microspheres containing rifampicin in alveolar macrophages. *Colloids Surf. B. Biointerfaces* 76, 151 **(2010)**.
62. K. Hirota, T. Hasegawa, H. Hinata, F. Ito, H. Inagawa, C. Kochi, G. I. Soma, K. Makino, and H. Terada, Optimum conditions for efficient phagocytosis of rifampicin-loaded PLGA microspheres by alveolar macrophages. *J. Control. Release* 119, 69 **(2007)**.
63. K. Hirota, T. Hasegawa, T. Nakajima, K. Makino, and H. Terada, Phagostimulatory effect of uptake of PLGA microspheres loaded with rifampicina on alveolar macrophages. *Colloids Surf. B Biointerfaces* 87, 293 **(2011)**.
64. M. Dutt and G. K. Khuller, Liposomes and PLG microparticles as sustained release antitubercular drug carriers—an *in vitro–in vivo* study. *Int. J. Antimicrob. Agents.* 18, 245 **(2001)**.
65. K. Makino, N. Yamamoto, K. Higuchi, N. Harada, H. Ohshima, and H. Terada, Phagocytic uptake of polystyrene microspheres by alveolar macrophages: Effects of the size and surface properties of the microspheres. *Colloids Surf. B Biointer.* 27, 33 **(2003)**.
66. E. Almouazen, S. Bourgeois, A. Boussaïd, P. Valot, C. Malleval, H. Fessi, S. Nataf, and S. Briançon, Development of a nanoparticle-based system for the delivery of retinoic acid into macrophages. *Int. J. Pharm.* 430, 207 **(2012)**.
67. A. V. Chavez-Santoscoy, R. Roychoudhury, N. L. B. Pohl, M. J. Wannemuehler, B. Narasimhan, and A. E. Ramer-Tait, Tailoring the immune response by targeting *C*-type lectin receptors on alveolar macrophages using "pathogen-like" amphiphilic polyanhydride nanoparticles. *Biomaterials* 33, 4762 **(2012)**.
68. M. K. Yoo, I. Y. Park, I. Y. Kim, I. K. Park, J. S. Kwon, H. J. Jeong, Y. Y. Jeong, and C. S. Cho, Superparamagnetic iron oxide nanoparticles coated with mannan for macrophage targeting. *J. Nanosci. Nanotechnol.* 8, 5196 **(2008)**.
69. T. Hasegawa, K. Iijima, K. Hirota, T. Nakajima, K. Makino, and H. Terada, Exact determination of phagocytic activity of alveolar macrophages toward polymer microspheres by elimination of those attached to the macrophage membrane. *Colloids Surf. B Biointer.* 63, 209 **(2008)**.